Erythrocyte-derived microvesicles induce arterial spasms in JAK2V617F myeloproliferative neoplasm

Johanne Poisson, … , Chantal M. Boulanger, Pierre-Emmanuel Rautou
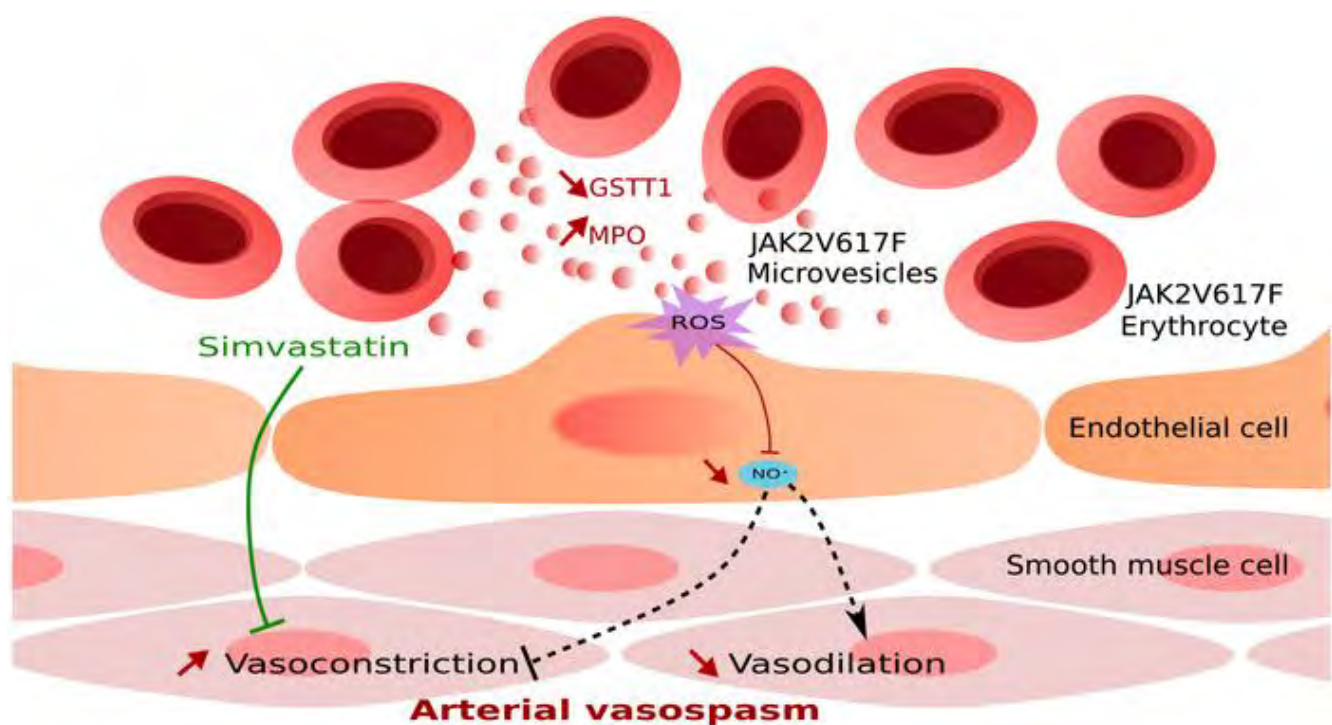
Research   In-Press Preview   Cardiology   Hematology

Graphical abstract

Find the latest version:

https://jci.me/124566/pdf

Title: Erythrocyte-derived microvesicles induce arterial spasms in *JAK2*[V617F] myeloproliferative neoplasm

Authors: Johanne Poisson[1,2,3], Marion Tanguy[1,2], Hortense Davy[1], Fatoumata Camara[1], Marie-Belle El Mdawar[1], Marouane Kheloufi[1], Tracy Dagher[4], Cécile Devue[1], Juliette Lasselin[1], Aurélie Plessier[5,6], Salma Merchant[4], Olivier Blanc-Brude[1], Michèle Souyri[7], Nathalie Mougenot[8], Florent Dingli[9], Damarys Loew[9], Stephane N. Hatem[10], Chloé James[11,12,13], Jean-Luc Villeval[4], Chantal M. Boulanger[1], Pierre-Emmanuel Rautou[1,2,4,5]∗

Affiliations:

[1] Université de Paris, PARCC, Inserm, Paris, France

[2] Université de Paris, Centre de recherche sur l'inflammation, Inserm, Paris, France

[3] Geriatrics Department, Hôpital Européen Georges Pompidou, AP- HP, Paris, Île-de-France, France

[4] Inserm U1170, Institut Gustave Roussy, University Paris XI, Villejuif, France

[5] Service d'Hépatologie, DHU Unity, Pôle des Maladies de l'Appareil Digestif, Hôpital Beaujon, AP-HP, Clichy, France

[6] Centre de Référence des Maladies Vasculaires du Foie, French Network for Rare Liver Diseases (FILFOIE), European Reference Network (ERN) 'Rare-Liver'

[7] Inserm UMR-S1131, IHU, Université de Paris, Paris, France

[8] Sorbonne University, INSERM UMS 28, Phénotypage du petit animal, Plateform PECMV, Paris, France

[9] Laboratoire de Spectrométrie de Masse Protéomique, Institut Curie, Université de recherche PSL, F75248, Paris, France

[10] Sorbonne University, INSERM, UMR1166, Institute of Cardiometabolism and Nutrition (ICAN), Paris, France

[11] Inserm, Biology of Cardiovascular, U1034, Pessac, France

[12] University of Bordeaux, Pessac, France

[13] Laboratory of Hematology, Bordeaux University Hospital Center, Pessac, France

30   *Correspondence to:

Prof. Pierre-Emmanuel RAUTOU, MD PhD

Service d'Hépatologie, Hôpital Beaujon,

Assistance Publique-Hôpitaux de Paris, Clichy, France

Telephone: +33 1 71 11 46 79

35   Fax: + 33 1 40 87 55 30

E-mail: pierre-emmanuel.rautou@inserm.fr

Conflict of interest statement: The authors have declared that no conflict of interest exists.

40

Abstract:

Arterial cardiovascular events are the leading cause of death in patients with $JAK2^{V617F}$ myeloproliferative neoplasms (MPN). However, their mechanisms are poorly understood. The high prevalence of myocardial infarction without significant coronary stenosis or atherosclerosis in patients with MPN suggests that vascular function is altered. Consequences of $JAK2^{V617F}$ mutation on vascular reactivity are unknown. We observe here increased responses to vasoconstrictors in arteries from $Jak2^{V617F}$ mice, resulting from disturbed endothelial nitric oxide pathway and increased endothelial oxidative stress. This response was reproduced in wild-type mice by circulating microvesicles isolated from patients carrying $JAK2^{V617F}$ and by erythrocyte-derived microvesicles from transgenic mice. Microvesicles of other cellular origins had no effect. This effect was observed ex vivo on isolated aortas, but also in vivo on femoral arteries. Proteomic analysis of microvesicles derived from $JAK2^{V617F}$ erythrocytes identified increased expression of myeloperoxidase as the likely mechanism accounting for microvesicles effect. Myeloperoxidase inhibition in microvesicles derived from $JAK2^{V617F}$ erythrocytes supressed their effect on oxidative stress. Antioxidants, such as simvastatin and N-acetyl-cysteine, improved arterial dysfunction in $Jak2^{V617F}$ mice.

In conclusion, $JAK2^{V617F}$ MPN are characterized by exacerbated vasoconstrictor responses resulting from increased endothelial oxidative stress caused by circulating erythrocyte-derived microvesicles. Simvastatin appears as promising therapeutic strategy in this setting.

Main Text:

Introduction

65   Bcr/Abl-negative myeloproliferative neoplasms (MPNs) are clonal hematopoietic stem cell disorders characterized by the proliferation of particular hematopoietic lineages without blockage in cell maturation. They include polycythemia vera, essential thrombocythemia, and primary myelofibrosis *(1)*. *JAK2* is the most common MPN driver gene. *JAK2^{V617F}* is a gain of function mutation leading to growth factors hypersensitivity, detected in around 70% of MPNs (95% in

70   polycythemia vera and 50% to 60% in essential thrombocythemia and pre-primary myelofibrosis / primary myelofibrosis) *(1)*. *JAK2^{V617F}* appears in pluripotent hematopoietic progenitor cells and is present in all erythroid and myeloid lineages *(1)*. In addition, several groups described *JAK2^{V617F}* in endothelial cells in the liver and the spleen of patients with splanchnic vein thrombosis *(2, 3)* and in circulating endothelial progenitor cells (4–6).

75   Cardiovascular diseases (CVD) reveal MPNs in about 30% of the patients and are the first cause of morbidity and mortality in these patients *(7)*. Arterial events represent 60-70% of these cardio-vascular events *(7)*. Interestingly, myocardial infarction without significant coronary stenosis by angiography was observed in 21% of patients with MPN *(8)* versus only 3% in a similar population without MPN *(9)*. This observation prompted the European society of cardiology to

80   recommend searching for MPNs in case of myocardial infarction without obstructive coronary artery disease *(10)*. The mechanism underlying this link between myocardial infarction without obstructive coronary artery disease and MPNs is unknown, but vasoactive phenomenon (local intense vasoconstriction) can be suspected *(11, 12)*.

      Therefore, the purpose of the present study was to examine the consequences of *JAK2^{V617F}*

85   mutation on arterial vascular reactivity.

Results

Increased arterial contraction in mice carrying Jak2^{V617F} in hematopoietic and endothelial cells

As *JAK2^{V617F}* is present in both hematopoietic and endothelial cells in patients with MPN *(2, 3)*, we first investigated vasoactive response in a mouse model mimicking the human disease. We generated mice expressing JAK2^{V617F} in hematopoietic and in endothelial cells by crossing *Jak2$^{V617F\ Flex/WT}$* mice with *VE-Cadherin-cre* mice. *VE-Cadherin* being expressed during early embryonic life in a precursor of both endothelial and hematopoietic cells *(13)*, *Jak2$^{V617F\ Flex/WT}$;VE-Cadherin-cre,* thereafter referred to as *Jak2^{V617F} HC-EC,* developed as expected a MPN, attested by higher spleen weight (2.3 to 5.7 % of body weight *vs.* 0.3 to 0.6 % for littermate controls, p<0.0001), and higher haemoglobin level, platelet and white blood cell counts than littermate controls (Figure 1A-D). The endothelial and hematopoietic progenitor cells recombination was verified by crossing *VE-Cadherin-cre* with *mTmG* mice (Figure S1).

By performing myography assay, we observed ex vivo that aortas from *Jak2^{V617F} HC-EC* mice displayed a major increase in the response to phenylephrine (Figure 1E), but also to potassium chloride (Figure 1F) and to angiotensin II (Figure 1G), as compared with littermate controls. Removing the endothelium suppressed this increased arterial contraction (Figure 1H). Likewise, we observed in vivo that femoral arteries from *Jak2^{V617F} HC-EC* mice displayed an increased response to phenylephrine as compared with littermate controls (Figure 1I). Thus, *Jak2^{V617F}* in endothelial and hematopoietic cells strongly increases arterial response to vasoconstrictors in an endothelium-dependent manner.

Because of the high rate of myocardial infarction without significant coronary stenosis reported in patients with MPN *(8)*, we investigated cardiac vascular bed by performing electrocardiography in *Jak2^{V617F} HC-EC* mice and their littermate controls. After intravenous

injection of phenylephrine $Jak2^{V617F}$ HC-EC mice displayed electrocardiogram modifications including bradycardia and arrhythmia, that are indirect signs of coronary spasm *(14)* (Figure 1J-K).

115   ***Increased arterial contraction in mice with JAK2^{V617F} specifically expressed in hematopoietic cells but not in endothelial cells***

To determine if this increased arterial contraction was due to JAK2^{V617F} in endothelial cells or in hematopoietic cells, we first generated mice expressing JAK2^{V617F} only in endothelial cells. We crossed *Jak2$^{V617F\ Flex/WT}$* mice with inducible *VE-Cadherin-cre-ERT2* mice expressing the cre

120   recombinase after tamoxifen injection only in endothelial cells. As expected, *Jak2$^{V617F\ Flex/WT}$; VE-Cadherin-cre-ERT2 (*thereafter referred to as *Jak2^{V617F} EC*) mice did not develop MPN (Figure 2A-D). Adequate endothelial recombination was verified by crossing *VE-Cadherin-cre-ERT2* mice with *mTmG* mice (Figure S1). We previously demonstrated the absence of hematopoietic recombination in this model *(15)*. We observed no difference in arterial response to phenylephrine

125   between the *Jak2^{V617F} EC* mice and littermate controls (*Jak2^{WT})* (Figure 2E).

To assess the implication of JAK2^{V617F} in hematopoietic cells, we generated mice expressing *Jak2^{V617F}* only in hematopoietic cells, by transplanting lethally irradiated C57BL/6 mice with *Jak2^{V617F}* bone marrow cells obtained from *Jak2^{V617F} HC-EC* mice. Irradiated C56BL/6 mice transplanted with *Jak2^{WT}* BM were used as controls. Hematopoietic expression of JAK2^{V617F}

130   induced a MPN (Figure 2F-I) and an increased arterial response to phenylephrine (Figure 2J). Taken altogether, these findings demonstrate that presence of the *Jak2^{V617F}* mutation in hematopoietic, but not in endothelial cells, is responsible for the increase in arterial contraction in response to vasoconstrictors we observed in *Jak2^{V617F} HC-EC* mice (Figure 1E-G).

Increased arterial contraction induced by microvesicles from JAK2^{V617F} patients

We then sought to identify the mediators responsible for the increased response to vasoconstrictors when JAK2^{V617F} was present in hematopoietic cells and tested the hypothesis that circulating blood might convey biological information from hematopoietic cells to the vascular wall. Circulating microvesicles, *i.e.* extracellular vesicles having a size ranging from 0.1 to 1 μm, are now recognized as triggers of various types of vascular dysfunction *(16)*. We therefore examined the effect of circulating microvesicles isolated from the blood of patients with MPN on vascular responses to vasoactive agents. We isolated plasma microvesicles from 7 patients carrying JAK2^{V617F} (2 males, 5 females; blood drawn before introduction of cytoreductive therapy), and from 5 healthy controls (2 males, 3 females; age not significantly different from patients). We incubated these microvesicles at their plasma concentration with aortic rings from wild type mice and observed that plasma microvesicles from patients carrying JAK2^{V617F} reproduced the increased response to phenylephrine (Figure 3A). Plasma without microvesicles from the same patients and controls had no effect (data not shown).

Increased arterial contraction induced by erythrocytes-derived microvesicles from Jak2^{V617F} mice

We then sought to determine the subpopulation of microvesicles responsible for this increased arterial contraction. We generated microvesicles from each type of blood cells from *Jak2^{V617F} HC-EC* mice or littermate controls and incubated these microvesicles, at the same concentration, with aortic rings from wild type mice. Erythrocyte-derived microvesicles generated from *Jak2^{V617F} HC-EC* mice reproduced the increased response to phenylephrine on aortic rings ex vivo (Figure 3E), while platelet, peripheral blood mononuclear cell and polynuclear neutrophil microvesicles did not (Figure 3B-D). Likewise, in vivo*,* femoral arteries from wild-type mice

injected with microvesicles derived from JAK2^{V617F} erythrocytes displayed an increased response to phenylephrine as compared with wild-type mice injected with microvesicles derived from littermate controls' erythrocytes (Figure 3F). Microvesicles generated from *Jak2^{V617F} HC-EC* mice erythrocytes carried *Jak2^{V617F}* mRNA (Figure 3G). To investigate the interaction of erythrocyte-derived microvesicles with endothelial cells, we labeled microvesicles with the fluorescent dye PKH-26, incubated them with endothelial cells and then performed confocal microscopy on endothelial cells. Fluorescence was detected in endothelial cells, suggesting that erythrocyte-derived microvesicles were taken-up by endothelial cells (Figure 3H, I) (17). No difference in uptake was observed between microvesicles from *Jak2^{V617F} HC-EC* erythrocytes and their wild-type counterparts (Figure 3H, I).

We then wanted to determine whether the increased number of erythrocytes could in itself explain this effect or if qualitative changes were involved. We generated a mouse model of polycythaemia without *Jak2^{V617F}*, caused by chronic epoietin injections. After 3 weeks of epoietin treatment, haemoglobin reached a level similar to that of *Jak2^{V617F} HC-EC* mice (18.5 g/dL, interquartile range 16.5-19.5, *vs.* 17.6 g/dL, interquartile range 15.7-19.7, respectively; n=5 and n=13 respectively; p=0.67). However, this model with high number of circulating erythrocytes failed to reproduce the increased response to phenylephrine observed in *Jak2^{V617F} HC-EC* mice aortas (Figure 3J). Thus, the presence of the *Jak2^{V617F}* mutation in erythrocyte-derived microvesicles is required to cause increased arterial contraction.

NO pathway inhibition and endothelial increased oxidative stress status

We then investigated how microvesicles derived from JAK2^{V617F} erythrocytes increase response to vasoconstrictive agents.

We examined first the nitric oxide (NO) pathway. We observed ex vivo on aortas and in vivo on femoral arteries that *Jak2^{V617F} HC-EC* mice, reproducing the human disease, display an impaired dilatation to acetylcholine (Figure 4A, B). This impaired dilatation capacity was not due to decreased sensitivity to NO of vascular smooth muscle cells, as the response to a direct NO-donor (SNAP) was not different between *Jak2^{V617F} HC-EC* mice and littermate controls, both ex vivo and in vivo (Figure 4C, D). We also observed that, after pre-incubation with the NO synthase (NOS) inhibitor L-Name, aorta from *Jak2^{V617F} HC-EC* mice had a similar response to phenylephrine as littermate controls (Figure 4E). Therefore, these results demonstrate that the increased arterial contraction observed in *Jak2^{V617F} HC-EC* mice results from a dysfunctional endothelial NO pathway.

Because previous works showed that heme in erythrocytes microvesicles can scavenge NO [18, 19], we quantified heme in microvesicles derived from *Jak2^{V617F} HC-EC* mice and control mice erythrocytes, but observed no difference (Figure S2).

We then investigated generation of reactive oxygen species, *i.e.* inhibitors of NOS activity and NO bioavailability [20] and demonstrated 4 times more reactive oxygen species in the aortic endothelium of *Jak2^{V617F} HC-EC* mice than in littermate controls (Figure 4F, G). Conversely, reactive oxygen species generation was normal in the aortic endothelium of *Jak2^{V617F} EC* mice, expressing JAK2^{V617F} only in endothelial cells (Figure 4H, I). Likewise, aortic endothelium from wild-type mice injected with microvesicles derived from JAK2^{V617F} erythrocytes displayed more reactive species generation than aortic endothelium of mice injected with microvesicles derived from littermate controls erythrocytes (Figure 4 J, K). There was no reactive oxygen species generation in underlying smooth muscle cells in any of these experiments (data not shown). Altogether, these results show that microvesicles derived from JAK2^{V617F} erythrocytes induce an excessive oxidative stress in endothelial cells leading to a decreased availability of NO.

To ascertain the implication of the increased oxidative stress in the increased arterial contraction in *Jak2^{V617F} HC-EC* mice, we treated these mice with N-Acetyl-Cysteine (NAC, activator of glutathione pathway and anti-oxidant) for 14 days intraperitoneally. This treatment had no effect on blood cell count or spleen weight (Figure S4) but normalized arterial contraction to phenylephrine (Figure 4L).

Increased endothelial oxidative stress status by myeloperoxidase in erythrocyte-derived microvesicles from Jak2^{V617F} mice

To shed light on the mechanisms underlying this increased oxidative stress induced by microvesicles derived from JAK2^{V617F} erythrocytes, we performed a proteomic analysis of these microvesicles (data are available via ProteomeXchange with identifier PXD014451). All proteins involved in reactive oxygen species detoxification or generation are shown in the volcano-plot shown in Figure 4L and their role in oxidative stress summarized in Table S1. We found one protein significantly deregulated (glutathione S transferase theta 1, GSTT1) and one protein only detected in microvesicles derived from JAK2^{V617F} erythrocytes (myeloperoxidase, MPO) that could explain the observed effect (Figure 5A). We also considered cytochrome b-245 heavy and light chain (NOX2) although only few peptides were detected in microvesicles derived from JAK2^{V617F} erythrocytes (1 peptide of heavy chain in 1/6 samples and 1 peptide of light chain in 2/6 samples), since NOX plays a key role in oxidative stress and since no NOX2 peptide was detected in microvesicles derived from JAK2^{WT} erythrocytes. Western blot analyses were then performed on microvesicles derived from JAK2^{V617F} and control erythrocytes to verify proteomic results. By western blot, NOX2 expression evaluated by Gp91 was not significantly different between JAK2^{V617F} and controls erythrocyte-derived microvesicles (Figure S3). GSTT1, which has an anti-oxidant effect *(21)*, was significantly lower in JAK2^{V617F} than in control erythrocyte-

derived microvesicles (Figure 5B, C). Expression of MPO, a protein with a strong pro-oxidant effect *(22)* was much higher in JAK2^{V617F} than in control erythrocyte-derived microvesicles (Figure 5D, E). We then directly inhibited MPO in microvesicles derived from erythrocytes of *Jak2^{V617F} HC-EC* mice before incubation with endothelial cells (HUVEC) in vitro. We observed that the MPO inhibitor (PF06281355) completely reversed the increase in endothelial oxidative stress induced by *Jak2^{V617F}* erythrocyte-derived microvesicles (Figure 5F, G).

In conclusion, JAK2^{V617F} erythrocyte-derived microvesicles carry MPO that confers a pro-oxidant phenotype to endothelial cells, leading to increased arterial contraction observed in *Jak2^{V617F} HC-EC* mice.

Statins as a potential new treatment in myeloproliferative neoplasms

We then tested if available treatments for MPNs, namely hydroxyurea and ruxolitinib, affect this increased arterial contraction. In *Jak2^{V617F} HC-EC* mice, best representing the human disease, hydroxyurea for 10 consecutive days decreased spleen weight, haemoglobin level and white blood cell count (Figure 6A, B, D). However, platelet count was not affected by this short time hydroxyurea treatment (Figure 6C). Hydroxyurea significantly improved contraction in response to phenylephrine as compared to vehicle (Figure 6E).

We then treated *Jak2^{V617F} HC-EC* mice with ruxolitinib for 21 consecutive days and observed a significant decrease in the spleen weight and white blood cell count (Figure 6F, I), but no effect on the haemoglobin level and on platelet count (Figure 6G, H). Ruxolitinib had no effect on arterial response to phenylephrine (Figure 6J).

Beyond its lowering cholesterol effect, simvastatin also improves endothelial function through NO pathway and by preventing oxidative stress damage *(23, 24)*. Thus, we tested its effect on arterial response to phenylephrine in *Jak2^{V617F} HC-EC* mice. Fourteen days of treatment with

simvastatin did not change spleen weight, haemoglobin level or platelet count (Figure 6 K-M). There was only a slight decrease in white blood cells count following simvastatin treatment (Figure 6N). Interestingly, simvastatin significantly improved aortic response to phenylephrine as compared to vehicle (Figure 6O).

Discussion

This study demonstrated that JAK2^{V617F} erythrocyte-derived microvesicles carrying MPO, are responsible for an increased oxidative stress in arterial endothelium and a decreased availability of NO, which strongly increased arterial contraction to vasoconstrictive agents, possibly accounting for arterial events associated with MPNs. Simvastatin, a drug with anti-oxidant properties, improved arterial contraction.

The first major finding of our study is the demonstration that *JAK2^{V617F}* MPN induces a considerable increase in arterial contraction. This finding suggests a vasospastic phenomenon associated with MPN and thus represents a paradigm shift in MPNs where arterial events were only seen as a result of a thrombotic process *(7)*. Our results obtained ex vivo and in vivo could explain this higher incidence of arterial events in patients with polycythemia vera than in the general population and the high prevalence of myocardial infarction without significant coronary stenosis by angiography in patients with MPN *(8)*. Arterial spasm is an underdiagnosed phenomenon that can happen in patients without atherosclerosis but is also favoured by underlying non-stenotic atherosclerotic plaques. This suggests that the effect we observed might not only account for myocardial infarction without significant coronary stenosis reported in patients with MPN, but might also more widely favour arterial events in patients with atherosclerotic plaques and MPN *(11, 12)*. Moreover, arterial spasm not only occurs in coronary arteries, but also in brain arteries *(25)*. We also found an impairment in arterial dilatation, which is in line with the altered

endothelial dependant flow mediated vasodilatation reported in patients with polycythemia vera, in the absence of overt arterial disease *(26)*.

280

The second major finding of our work is the contribution of JAK2^{V617F} erythrocyte-derived microvesicles to this increased arterial contraction associated with MPN. Importantly, we observed this effect with JAK2^{V617F} erythrocyte microvesicles from mice, but also with microvesicles isolated from patients carrying JAK2^{V617F}. We thus highlight here a crucial vascular role of

285 microvesicles in MPNs, beyond their so far described implication in coagulation in this setting (27–31). Although patients with MPNs have higher circulating levels of microvesicles than healthy individuals, we assessed vascular reactivity using the same concentrations of microvesicles for both groups, suggesting that microvesicles composition, and not concentration, accounts for the observed vascular effect (27, 28, 32–35). We cannot rule out the fact that JAK2^{V617F} erythrocytes

290 themselves, in addition to microvesicles, could also directly increase arterial contraction associated with MPNs.

Finally, in our work we demonstrated that NO pathway inhibition and increased endothelial oxidative stress are implicated in this increased arterial contraction in MPN. Several groups

295 reported high levels of circulating reactive oxygen species products (36–38) and low antioxidant status in MPN *(37, 39)*, but endothelial oxidative stress had never been investigated. Erythrocyte microvesicles have already been linked to vascular dysfunction in different settings, such as erythrocytes storage or sickle cell disease *(18, 19, 40)*, but never in the context of MPN. Thanks to proteomics approaches we were able to identify a defect in GSTT1 and an over expression of

300 MPO in microvesicles derived from JAK2^{V617F} erythrocytes. Using a direct and irreversible inhibition of MPO, we were able to ascertain the role of MPO carried by microvesicles derived

from JAK2^{V617F} erythrocytes in the increase endothelial oxidative stress. MPO is a polycationic heme-containing glycoprotein stored mainly in the azurophilic granules of neutrophils, but up to 30% of total cellular MPO can be released as active enzyme into the extracellular space. Interestingly, extra-cellular MPO can bind to red blood cells membrane and favours endothelial dysfunction in the context of ischemic heart disease (41–45). Our results demonstrate that MPO binds to erythrocyte-derived microvesicles, increases endothelial oxidative stress and vascular response to vasoconstrictors.

The role of GSTT1 in the increased endothelial oxidative stress status and vascular reactivity we observed with microvesicles derived from JAK2^{V617F} erythrocytes remains uncertain, because we could not restore a normal level of GSTT1 only in microvesicles. The normalisation of vascular reactivity induced by NAC could be explained by the glutathione inducer activity of NAC, but could also just be due to the potent anti-oxidant activity of this drug.

In addition to demonstrating how *JAK2^{V617F}* induces this increased arterial contraction, our results open new potential therapeutic perspectives to prevent cardio-vascular events in patients with MPN. We demonstrated that simvastatin, a well-known and easily accessible drug, strongly improves arterial response to vasoconstrictive agent in our MPN mouse model. These results thus pave the way for testing simvastatin to prevent arterial events in patients with MPN. We also tested available treatments for MPN and observed that hydroxyurea, but not ruxolitinib, improved arterial contraction. This difference might be explained by the fact that hydroxyurea decreased erythrocyte count in our mouse model whereas ruxolitinib did not *(46, 47)*.

In conclusion, our study showed that microvesicles derived from erythrocytes are responsible for an increased arterial contraction in *JAK2^{V617F}* MPNs. This effect is due to an overexpression of MPO in JAK2^{V617F} erythrocyte-derived microvesicles, which is responsible for

an increased endothelial oxidative stress and a NO pathway inhibition. Simvastatin appears as an original new approach to prevent arterial events in MPN and warrants further studies.

Materials and Methods

Experimental design

The objective of our study was to analyse endothelial reactivity in MPN. We first noticed a major increase in arterial contraction in *Jak2^{V617F} HC-EC* mice, a model with *Jak2^{V617F}* expression both in hematopoietic and endothelial cells, that mimics the human disease. We then created mouse models specifically mutated in endothelial or in hematopoietic cells. We then searched for the mediators responsible for the increased response to vasoconstrictors when *Jak2^{V617F}* was present in hematopoietic cells and tested the hypothesis that circulating blood might convey biological information from hematopoietic cells to the vascular wall and focused on microvesicles. We identified that erythrocyte-derived microvesicles were responsible for this effect and performed a mass spectrography analysis to highlight the proteins involved. Sample size was chosen based on previous works using the same technique (myography) and microvesicles, published by our team *(48, 49)*.

Mouse breeding occurred in our animal facility in accordance with the local recommendations. Control mice were littermate, appropriate, age, sex and genetic background, matched to account for any variation in data. Institutional animal care and use committee at INSERM (Descartes university, Paris, France) approved all animal experiments (CEEA-17053).

Number of experimental replicates is provided in each figure legend and included at least 3 independent experiments. For each myography experiment, duplicates with the same aorta were used, averaged and counted as n=1. There was no randomization in these experiments. We did not exclude any other sample than those not fulfilling the quality criteria detailed in the corresponding

15

350   methods section. Only aorta with a viable endothelium were used for myography (see

corresponding methods section for criteria).

For human samples, inclusion and exclusion criteria were defined prior to sample collection (see

corresponding methods section for criteria). No outlier was excluded. Investigators were not

blinded to group allocation during collection and analysis of the data. All patients (carrying

355   *JAK2^{V617F}* with a past history of splanchnic vein thrombosis, not receiving any specific treatments

other than vitamin-k antagonists) and healthy volunteers gave writing consent to the study. Human

study was performed in accordance with the ethical guidelines of the 1975 Declaration of Helsinki

and was approved by the institutional review board Bichat-Claude-Bernard (Paris; France).

360   ***Murine models***

All mice were on a C57BL/6 background. Mice carrying constitutive *Jak2^{V617F}* mutation in

endothelial and hematopoietic cells were obtained by crossing *VE-cadherin-Cre* transgenic mice

provided by M. Souyri *(13)* with *Jak2$^{V617F\ Flex/WT}$* mice provided by M. Villeval *(50)*. Mice carrying

inducible *JAK2^{V617F}* mutation specifically in endothelial cells were obtained by crossing *VE-*

365   *Cadherin-cre-ERT2* transgenic mice provided by R. Adams *(51)* with *Jak2$^{V617F\ Flex/WT}$* mice

provided by M. Villeval *(50)*. The Flex (for Flip-Excision) strategy allows the expression of a

mutated gene in adulthood, in a temporal and tissue-specific manner *(52)*. It allows an efficient

and reliable Cre-mediated genetic switch: the expression of a given gene is turned on by inversion,

while expression of another one is simultaneously turned off by excision. In all experiments, male

370   and female mice were used.

For organ chamber experiments and femoral in vivo experiments, mice were euthanized

between the ages of 8 and 17 weeks. For induction of Cre recombinase expression in *Jak2^{V617F}*

$^{Flex/WT}$;VE-Cadherin-cre-ERT2 mice, mice were injected intraperitoneally with tamoxifen (Sigma,

T5648)*,* 1 mg/mouse/day for 5 consecutive days over 2 consecutive weeks (10 mg in total per
mouse) between the ages of 5 to 7 weeks. Experiments were performed between 4 to 6 weeks after
the last tamoxifen injection. Both female and male were used for each experiment.

Experiments were conducted according to the French veterinary guidelines and those
formulated by the European community for experimental animal use (L358-86/609EEC) and were
approved by the French ministry of agriculture (n° A75-15-32).

Verification of the efficient endothelial recombination in mouse models

All mice were on a C57BL/6 background. Mice with the *mTmG* reporter provided by C. James
(Inserm 1034) were crossed with *VE-cadherin-Cre* transgenic mice provided by M. Souyri or *VE-Cadherin-cre-ERT2* transgenic mice provided by R. Adams *(51)*. For induction of *mTmG;VE-Cadherin-cre-ERT2* model, mice were injected intraperitoneally with tamoxifen (Sigma, T5648)*,*
1 mg/mice/day for 5 consecutive days over 2 consecutive weeks (10 mg in total per mice) between
the ages of 5 to 7 weeks, and experiments were performed 2 weeks after the last injection of
tamoxifen. Aortas and femurs were harvested under isoflurane anaesthesia and fixed in 4% PFA.
Aorta were mounted "*en face*" on glass slides, while femurs were cryosectioned. All tissues were
imaged using a Leica SP5 confocal microscope (Leica) at 400 X magnification. For flow cytometry
analysis in Cre;mT/mG mice, bone marrow cells were stained with TER-119 APC and Gr-1 APC
(553673, Becton Dickinson) and analyzed on an Accuri C6 flow cytometer (BD Biosciences). Data
were interpreted using BD Accuri C6 Analysis Software.

Patient's inclusion

All patients fulfilling inclusion criteria were prospectively included at the Hepatology
department, Beaujon Hospital, Clichy, France, between May 2016 and July 2016. Only patients

carrying *JAK2^{V617F}* without specific treatment for MPNs were included. All patients had a past history of Budd-Chiari syndrome or portal vein thrombosis and were receiving vitamin K antagonists. Controls were healthy voluntaries. All patients and controls gave written consent to the study. This study was performed in accordance with the ethical guidelines of the 1975 Declaration of Helsinki and was approved by our institutional review board (CPP Ile de France IV, Paris; France).

Organ Chamber Experiments

Thoracic aortas from adult mice were isolated after animal sacrifice under 2% isoflurane anaesthesia. The aortic rings were mounted immediately in organ chambers (Multi WireMyograph system, model 610 M; Danish Myo Technology, Aarhus, Denmark) filled with Krebs–Ringer solution (NaCl 118.3 mmol/L, KCl 4.7 mmol/L, $MgSO_4$ 1.2 mmol/L, KH_2PO_4 1.2 mmol/L, $CaCl_2$ 1.25 mmol/L, $NaHCO_3$ 25.0 mmol/L and glucose 5.0 mmol/L) gassed with a mixture of O_2 95% and CO_2 5% (pH 7.4). The presence of functional endothelial cells was confirmed by the relaxation to acetylcholine chloride (Sigma, A6625) (10^{-5} mol/L) following a contraction evoked by phenylephrine (10^{-7} mol/L) and was defined as a relaxation $\geq$ 70% of the precontraction as previously described *(49)*. After extensive washout and equilibration, contraction to phenylephrine hydrochloride (concentration-response curve, 10^{-9} to 10^{-4} mol/L) (Sigma, P1250000) or angiotensin II (concentration-response curve, 10^{-9} to 10^{-6} mol/L) (Sigma, A9525) or KCL (80 mmol/L) and relaxation to acetylcholine chloride (concentration-response curve, 10^{-9} to 10^{-4} mol/L) or SNAP (S-Nitroso-N-acetyl-DL-penicillamine, Sigma, N3398) (concentration-response curve, 10^{-10} to 10^{-5} mol/L) were studied. For NO synthase inhibition, aorta rings were preincubated for 45 min with L-NAME 10^{-4} mol/L (Cayman, 80210) prior to concentration-response curve to phenylephrine without washout. In some experiments, the endothelium was

mechanically removed by inserting the tip of a pair of forceps within the lumen and by gently rubbing the ring back and forth on a piece of wet tissue. For the N-Acetyl-Cysteine experiment (NAC, commercial HIDONAC®, Zambon), NAC was added to the Krebs-Ringer solution at a final concentration of 20 mmol/L.

In vivo femoral reactivity

The femoral artery was carefully exposed from adult mice under 2% isoflurane anaesthesia. Krebs–Ringer solution (cf organ chamber experiment) gassed with a mixture of O_2 95% and CO_2 5% (pH 7.4) at 37° was permanently superfuse (2 mL/min) on the exposed artery. After a 15-minute equilibration, arterial responses were determined by addition of phenylephrine (10^{-3} mol/L) for 2 min then acetylcholine (10^{-1} mol/L) for 1 min (Sigma Chemical Co.). On the controlateral leg, with the same protocol, KCL (80 mmol/L) then SNAP (S-Nitroso-N-acetyl-DL-penicillamine, 10^{-3} mol/L) were used. All dilutions were prepared just before application. Changes in vessel diameter were continuously recorded on a videotape recorder. Subsequently, images were exported and vessel outer diameters were analyzed using Image J Software.

Isolation and characterization of patients' circulating microvesicles

Circulating microvesicles from patients or healthy control were isolated from platelet-free plasma obtained by successive centrifugations of venous blood, as reported previously *(53)*. Briefly, citrated venous blood (15 mL) was centrifuged twice at 2500g for 15 minutes (at room temperature) to remove cells and cell debris and to obtain platelet-free plasma (PFP). A portion of this PFP was then aliquoted and stored at -80°C. The rest was centrifuged at 20500g for 2 hours (4°C). Supernatant of this 20500g centrifugation was then discarded and the resulting microvesicles pellet was resuspended in a minimal volume of supernatant, aliquoted and stored at

-80°C. For each patient, concentrations of annexin V positive microvesicles were analysed in the PFP and the resuspended pellet of microvesicles.

Circulating levels of annexin V+ microvesicles (IM3614, BD) were determined on a Gallios flow cytometer (Beckman Coulter, Villepinte, France) using a technique previously described in detail *(49, 53)*.

450

Generation of microvesicles from mice

Blood samples were collected from the inferior vena cava of *Jak2^{V617F} HC-EC* mice or littermate controls using a 25 G x 1' needle in a 1 mL syringe pre-coated with 3.8% sodium citrate.

455 PFPs were generated as described above for patients and used to measure plasma annexin V positive microvesicles in mice. The pelleted cells obtained following the first 2500g centrifugation were resuspended in PBS to a final volume of 5 mL for control mice and 10 mL for *Jak2^{V617F} HC-EC* mice. PBMC, PMNC and erythrocytes were separated using a double percoll gradient (63% and 72% for control mice and 63% and 66% for *Jak2^{V617F} HC-EC* mice) using a 700g

460 centrifugation for 25 min, without brake. The slight differences between the protocols used for control and *Jak2^{V617F} HC-EC* mice are the results of the preliminary experiments we did to obtain pure isolation of each cell type. Cells were subsequently washed with PBS, then incubated with 5 µmol/L ionomycin TBS for 30min at 37°C to induce microvesicles generation. 5 mmol/L EDTA was then added to chelate free calcium. Cells were then discarded by centrifugations at 15000g for

465 1 min and the supernatants were collected. Microvesicles were isolated, as described above using a 20500g centrifugation during 45min. Concentrations of annexin V positive microvesicles (as described above) were analysed in the PFP and the 20500g microvesicles pellet for each mouse.

To isolate platelets, 500 µL of whole blood were diluted in 10 mL of PBS. A 1.063 g/mL density barrier was created by combining 5 mL of 1.320 g/mL 60% iodixanol stock solution

(OptiPrep density gradient medium, Sigma-Aldrich, Saint Louis, MO, USA) with 22 mL of diluent (0.85% NaCl, 20 mM HEPES-NaOH, pH 7.4, 1 mM EDTA). For platelet separation, 10 mL of each diluted blood were layered over 10 mL of density barrier and centrifuged at 350 g for 15 minutes at 20°C with the brake turned off. The interface between the density barrier and the blood contained platelets. Residual contaminating erythrocytes were removed by magnetic sorting. Briefly, the cell suspension was labelled with Anti-Ter-119 MicroBeads (Miltenyi Biotec ref 130-049-901) and erythrocytes (Ter-119+) were negatively sorted using a MACS® Separator. The remaining cells (platelets) were subsequently washed with PBS and exposed to 5 µmol/L ionomycin in TBS for 30 minutes at 37°C. 5 mM EDTA was then added to chelate free calcium. Finally, cells were discarded by centrifugation at 15000g for 1 minute, the supernatant was collected and microvesicles isolated, as previously described.

Vascular reactivity following exposure to microvesicles

For organ chamber experiments, thoracic aortas from adult C57BL/6 mice (8 to 10 weeks old) were isolated after sacrifice under isoflurane anaesthesia. Mouse aortic rings were incubated for 24 hrs; 37°C in a 5% CO_2 incubator, with filtered DMEM supplemented with antibiotics (100 IU/mL streptomycin, 100 IU/mL penicillin (Gibco, Invitrogen, Paisley, Scotland), and 10 µg/mL polymyxin B (Sigma, St Louis, MO) in the presence of microvesicles. Aortic rings were then mounted in organ chambers and concentration-response curves to pharmacological agents were performed.

For femoral artery in vivo experiment, C57BL/6 mice were injected intravenously (retro-orbital injection) with microvesicles (100 µL final volume with 2 µL heparin sodium (5000 IU/mL)). Experiments were performed 2 hours after injection.

Microvesicles from patients and healthy controls were incubated at their respective individual plasma concentration (Annexin-V positive microvesicles). Microvesicles generated from mice were incubated or injected at the same final concentration for *Jak2^{V617F} HC-EC* mice and control mice, namely 7000 Annexin V positive microvesicles / μL for erythrocyte and platelet-derived microvesicles and 700 Annexin V positive microvesicles / μL for PBMC and PMNC-derived microvesicles. We chose these concentrations since we found in preliminary experiments that the majority of mice have concentrations of Annexin V positive microvesicles between 1000 and 10000 / μL, and because PBMC and PMNC-derived microvesicles are consistently found less abundant in the blood than erythrocyte and platelet-derived microvesicles *(27, 32)*.

Bone marrow transplantation

We subjected 6 to 8 weeks old C57Bl/6J mice to medullar aplasia following 9.5 gray lethal total body irradiation. We repopulated the mice with an intravenous injection of bone marrow cells isolated from femurs and tibias of age matched *Jak2^{V617F} HC-EC* and of littermate control mice. Medullar reconstitution was allowed for 8 weeks before experiments.

Treatments

Hydroxyurea (Sigma, H8627), or the same volume of vehicle (NaCl 0.9%), was administrated for 10 consecutive days (100 mg/kg/day BID) by intra-peritoneal injections.

Ruxolitinib (Novartis) was administered for 21 consecutive days (30 mg/kg 2 times per day) by oral gavage *(54)*. Ruxolitinib was prepared from 15-mg commercial tablets in PEG300/5% dextrose mixed at a 1:3 ratio, as previously reported *(55)*. Control mice were administered the same volume of vehicle (PEG300/dextrose 5%).

Simvastatin (Sigma S6196) was administered for 14 days (20 mg/kg/day, once a day) by intra-peritoneal injections. Activation by hydrolysis was first achieved by dissolving 50 mg in 1 mL of pure ethanol and adding 0.813 ml of 1 mol/L NaOH. pH was adjusted to 7.2 by adding small quantities of 1 mol/L HCl and dilution was then performed in PBS *(56)*. Control mice were injected with the same volume of vehicle.

Human recombinant Epoietin alfa (5000 UI/kg, diluted in 0.2% BSA in PBS) or vehicle (0.2% BSA in PBS) was administered to wild type mice every 2 days for 3 weeks by intraperitoneal injection, as previously described *(57)*.

N-Acetyl-Cysteine (commercial HIDONAC, Zambon) diluted in NaCl 0.9% or the same volume of vehicle (NaCl 0.9%), was administrated for 14 consecutive days (500 mg/kg/day) by intraperitoneal injections.

Blood Cell count analysis

Blood was collected on the day of sacrifice from the inferior vena cava using a 25G x 1' needle in a 1 mL syringe pre-coated with 3.8% sodium citrate. Blood counts analyses were performed using a Hemavet 950FS analyser (Drew scientific).

Quantification of reactive oxygen species generation

Thoracic aortas from adult mice were isolated after animal sacrifice under 2% isoflurane anaesthesia, longitudinally opened and placed directly in HBSS (Hanks' balanced salt solution, Sigma, 14025-092). For each set of experiments, all aortas were processed immediately after removal, at the same time, with the same reagents and in the same manner. No plasma factor or blood cells were added during the ROS generation assessment. For positive and negative controls, 2 pieces of wild type aortas were incubated with H_2O_2 (100 µmol/L final concentration) for 20 min

540   at 37°C. For negative controls, N-Acetyl-Cysteine (5 mmol/L final concentration) was incubated

together with H_2O_2 for 20 min at 37°C. All aortas were then incubated with 5 µmol/L CellROX®

(Fisher scientific, C10422) for 30 min at 37°C. CellROX® Deep Red Reagent is a fluorogenic

probe designed to reliably measure reactive oxygen species inside living cells. The cell-permeable

CellROX® Deep Red dye is nonfluorescent while outside of the cell and in a reduced state and,

545   upon oxidation, exhibits excitation/emission maxima at 640/665 nm. After rinsing and fixation

(Paraformaldehyde 4%, 20 min), samples were costained with DAPI (0.1 µg/mL, Sigma) in order

to identify cell nuclei. After staining, aortas were washed with PBS, mounted "*en face*" on glass

slides and imaged using a bright field Zeiss Axio Imager Z1 (Zeiss) microscope. Images were

acquired in the 2 hours following staining at 400 X magnification. CellROX® positive surface (in

550   red) and the number of cells were quantified using Image J Software.

Myeloperoxidase inhibition in microvesicles

Erythrocyte-derived microvesicles from *Jak2^{V617F} HC-EC* mice were incubated for 1 hr

with an irreversible MPO inhibitor (MPOi, PF06281355, resuspended in DMSO, Sigma), diluted

555   in PBS (5 µmol/L final concentration). Then, the same amount of annexin V positive erythrocyte-

derived microvesicles (JAK2^{WT}, JAK2^{V617F} and JAK2^{V617F} with MPOi) were washed in PBS and

centrifuged at 20500g for 2 hrs. The pellet containing the microvesicles was then resuspended in

endothelial cell basic medium (Promocell). HUVECs (single donor, C-12200, lot 445Z011,

PromoCell) were then incubated for 2 hrs at 37°C with these microvesicles. At the end of the

560   incubation, and without washing cells, reactive oxygen species generation was assessed using

CELLROX® (Fisher scientific, C10422), as described above. After rinsing with medium and

paraformaldehyde (4%, 5 min), HUVECs were costained with DAPI (0.1 µg/mL, Sigma) in order

to identify nuclei. Images were acquired using a Confocal microscope, Leica SP8 at 400 X magnification.

565

Electrocardiography

Electrocardiograms were recorded from mice using the non-invasive ecgTUNNEL (Emka Technologies) with minimal filtering. Electrocardiogram was continuously monitored for 3 min (baseline). Waveforms were recorded using Iox Software and heart rate and intervals were measured with ECG Auto from recording traces. Following baseline determination, the animals received a single administration of phenylephrine (bolus, 3mg/Kg) by intravenous route at the caudal vein and electrocardiogram were recording 3-5 minutes more.

575 ### RNA gene allelic discrimination

Erythrocytes microvesicles were lysed with Qiazol lysis reagent (Qiagen) and RNA was extracted with RNeasy micro Kit (Qiagen) according to manufacturer's instructions. Dosage of RNA was performed with Qubit HS RNA assay Kit (ThermoFisher Scientitic). cDNA synthesis was performed with QuantiTect Reverse Transcription Kit (Qiagen). RNA gene allelic discrimination was performed by Taqman analysis with the ABI Prism GeneAmp 7500 Sequence Detection System (Applied Biosystem, Invitrogen) using as primers: TTTACAAATTCTTGAACCAGAATGTTC (JAK2 forward) and TTCTCACAAGCATTTGGTTTTGAAT (JAK2 reverse) and as probes: VIC-CTCCACAGACACAGAC-MGB for $JAK2^{WT}$ and 6-FAM-TCTCCACAGAAACAGAGA-MGB for $JAK2^{V617F}$.

Mass spectrometry analysis

Size-exclusion chromatography of microvesicles was then performed in order to separate microvesicles from soluble proteins. Successive aliquot of 150 μL were collected and measurement of protein absorbance was performed. Fractions contained in tubes 6 to 11, containing microvesicles, were selected and then centrifuged at 20 500g for two hours. To finish, microvesicles were lysed using a 1% triton buffer.

For mass spectrometry analysis, proteins were precipitated overnight at -20°C with 0.1 mol/L Ammonium Acetate glacial in 80% methanol (buffer 1). After centrifugation at 14000xg and 4°C for 15 min, the resulting pellets were washed twice with 100 μL of buffer 1 and further dried under vacuum (Speed-Vac concentrator). Proteins were then reduced by incubation with 10 μL of 5 mmol/L dithiotreitol (DTT) at 57°C for one hour and alkylated with 2 μL of 55 mmol/L iodoacetamide for 30 min at room temperature in the dark. Trypsin/LysC (Promega) was added twice at 1:100 (wt:wt) enzyme:substrate, at 37°C for 2 hrs first and then overnight. Samples were then loaded onto a homemade C18 StageTips for desalting. Peptides were eluted using 40/60 MeCN/H2O + 0.1% formic acid and vacuum concentrated to dryness. Online chromatography was performed with an RSLCnano system (Ultimate 3000, Thermo Scientific) coupled online to a Q Exactive HF-X with a Nanospay Flex ion source (Thermo Scientific). Peptides were first trapped on a C18 column (75 μm inner diameter × 2 cm; nanoViper Acclaim PepMap™ 100, Thermo Scientific) with buffer A (2/98 MeCN/H2O in 0.1% formic acid) at a flow rate of 2.5 μL/min over 4 min. Separation was then performed on a 50 cm x 75 μm C18 column (nanoViper Acclaim PepMap™ RSLC, 2 μm, 100Å, Thermo Scientific) regulated to a temperature of 50°C with a linear gradient of 2% to 30% buffer B (100% MeCN in 0.1% formic acid) at a flow rate of 300 nL/min over 91 min. MS full scans were performed in the ultrahigh-field Orbitrap mass analyzer in ranges m/z 375–1500 with a resolution of 120 000 at m/z 200. The top 20 intense ions were subjected to

Orbitrap for further fragmentation via high energy collision dissociation (HCD) activation and a resolution of 15 000 with the intensity threshold kept at 1.3×10^5. We selected ions with charge state from 2+ to 6+ for screening. Normalized collision energy (NCE) was set at 27 and the dynamic exclusion of 40s.

615   For identification, data were searched against the *Mus Musculus* one gene one protein (UP000000589_10090) UniProt database and a databank of the common contaminants using Sequest HF through proteome discoverer (version 2.2). Enzyme specificity was set to trypsin and a maximum of two-missed cleavage sites were allowed. Oxidized methionine and N-terminal acetylation were set as variable modifications. Maximum allowed mass deviation was set to 10

620   ppm for monoisotopic precursor ions and 0.02 Da for MS/MS peaks. The resulting files were further processed using myProMS *(58)* v3.6. FDR calculation used Percolator and was set to 1% at the peptide level for the whole study. The label free quantification was performed by peptide Extracted Ion Chromatograms (XICs) computed with MassChroQ version 2.2 *(59)*. For protein quantification, XICs from proteotypic peptides shared between compared conditions (TopN

625   matching) with two-missed cleavages were used. Median and scale normalization was applied on the total signal to correct the XICs for each biological replicate. To estimate the significance of the change in protein abundance, a linear model (adjusted on peptides and biological replicates) was performed and *p*-values were adjusted with a Benjamini–Hochberg FDR procedure with a control threshold set to 0.05.

630   The mass spectrometry proteomics data have been deposited to the ProteomeXchange Consortium via the PRIDE *(60)* partner repository with the dataset identifier PXD014451 (Username: reviewer44303@ebi.ac.uk and Password: yVaNmNXm).

Western Blot on erythrocyte-derived microvesicles

Erythrocyte-derived microvesicles generated as mentioned above were centrifuged at 20 500g for 2 hrs, and then lysed in 100 μL RIPA buffer containing 150 mmol/L NaCl, 50 mmol/L TrisHCl, pH 7.4, 2 mmol/L EDTA, 0.5% sodium deoxycholate, 0.2% sodium dodecyl sulfate, 2 mmol/L activated orthovanadate, complete protease inhibitor cocktail tablet (Complet mini, Roche, France) and complete phosphatase inhibitor cocktail tablet (Roche, France). Protein content was quantified using the Micro BCA Protein Assay Kit (Thermo Scientific). Equal loading was checked using Ponceau red solution. Membranes were incubated with primary antibodies (1/1000) (Anti-GP91, BD611415; Anti-GSTT1, Abcam199337; AntiMPO, Abcam45977). After secondary antibody incubation (anti-rat, Cell Signaling, 1/1000; anti-rabbit or anti-mouse, Amersham, GE Healthcare, UK 1/3000), immunodetection was performed using an enhanced chemiluminescence kit (Immun-Star Western C kit, Bio-Rad). Bands were revealed using the LAS-4000 imaging system. Values reported from Western blots were obtained by band density analysis using with ImageJ software and expressed as the ratio protein of interest compared to Ponceau.

Uptake of microvesicles by endothelial cells

Erythrocyte-derived microvesicles were stained with PKH26 dye (Sigma Aldrich) diluted in PBS, following manufacturer's instructions, washed in PBS and then centrifuged at 20500g for 2 hrs. The 20500g supernatant served for control experiments. Murine endothelial cells (the cell line called SVEC4-10, CRL-2181, lot 70008729, ATCC) were then incubated with these stained microvesicles or an equal volume of the 20500g supernatant. After 2 hrs at 37°C, cells were washed 3 times with DMEM (Gibco). Cells were then fixed in PFA 4% for 5 min, and then costained with DAPI (0.1 μg/mL, Sigma) in order to identify cell nuclei. Images were acquired using a Confocal microscope, Leica SP8 at 600 X magnification.

Statistics

For cumulative dose response curves, data were expressed as mean with standard error of the mean and compared using an analysis of variance for repeated measures. Other data were expressed as median with interquartile range (blood cell count and spleen weight) and compared using the Mann-Whitney U-test. All tests were 2 sided and used a significance level of 0.05. Data handling and analysis were performed with GraphPad Software, Inc.

Study approval

Institutional animal care and use committee at INSERM (Descartes university, Paris, France) approved all animal experiments (CEEA-17-053).

For human samples, inclusion and exclusion criteria were defined prior to sample collection (see corresponding methods section for criteria). All patients (carrying $JAK2^{V617F}$ with a past history of splanchnic vein thrombosis, not receiving any specific treatments other than vitamin-k antagonists) and healthy volunteers gave writing consent to the study. Human study was performed in accordance with the ethical guidelines of the 1975 Declaration of Helsinki and was approved by the institutional review board (CPP Ile de France IV, Paris; France).

Author Contributions: J.P., and P-E.R. designed the experiments and wrote the manuscript. J.P., H.D., F.C. performed myography experiments. J.P. performed oxidative stress experiments, M.T. generated microvesicles. J-L.V., C.J. and M.S. provided transgenic mice. M-B.E-M., C.D. and S.M. characterized the first mouse model. J.L. managed the mouse colony. M.K. performed *mTmG* experiments. A.P. included the patients and healthy controls. T.D performed JAK2^{V617F} qPCR on microvesicles. O.B.B analysed heme and haemoglobin content in microvesicles. S.N.H and N.M.

performed the electrocardiogram analysis. D.L. performed the mass spectrometry analysis. P-E.R. obtained funding for the project. All authors discussed and critically revised the manuscript.

References and Notes:

1. Vainchenker W, Kralovics R. Genetic basis and molecular pathophysiology of classical myeloproliferative neoplasms. *Blood* 2017;129(6):667–679.

2. Sozer S et al. The presence of JAK2V617F mutation in the liver endothelial cells of patients with Budd-Chiari syndrome. *Blood* 2009;113(21):5246–5249.

3. Rosti V et al. Spleen endothelial cells from patients with myelofibrosis harbor the JAK2V617F mutation. *Blood* 2013;121(2):360–368.

4. Rosti V et al. High Frequency of Endothelial Colony Forming Cells Marks a Non-Active Myeloproliferative Neoplasm with High Risk of Splanchnic Vein Thrombosis. *PLOS ONE* 2010;5(12):e15277.

5. Helman Ricardo et al. Granulocyte whole exome sequencing and endothelial JAK2V617F in patients with JAK2V617F positive Budd-Chiari Syndrome without myeloproliferative neoplasm. *British Journal of Haematology* 2018;180(3):443–445.

6. Teofili L et al. Endothelial progenitor cells are clonal and exhibit the JAK2(V617F) mutation in a subset of thrombotic patients with Ph-negative myeloproliferative neoplasms. *Blood* 2011;117(9):2700–2707.

7. Barbui T, Finazzi G, Falanga A. Myeloproliferative neoplasms and thrombosis. *Blood* 2013;122(13):2176–2184.

8. Pósfai É, Marton I, Borbényi Z, Nemes A. Myocardial infarction as a thrombotic complication of essential thrombocythemia and polycythemia vera. *Anatol J Cardiol* 2016;16(6):397–402.

9. Larsen AI et al. Characteristics and outcomes of patients with acute myocardial infarction and angiographically normal coronary arteries. *The American Journal of Cardiology* 2005;95(2):261–263.

10. Agewall S et al. ESC working group position paper on myocardial infarction with non-

obstructive coronary arteries. *Eur Heart J* 2017;38(3):143–153.

11. Davies MJ. The pathophysiology of acute coronary syndromes. *Heart* 2000;83(3):361–366.

12. Crea F, Libby P. Acute Coronary Syndromes: The Way Forward From Mechanisms to Precision Treatment. *Circulation* 2017;136(12):1155–1166.

13. Oberlin E, El Hafny B, Petit-Cocault L, Souyri M. Definitive human and mouse hematopoiesis originates from the embryonic endothelium: a new class of HSCs based on VE-cadherin expression. *Int. J. Dev. Biol.* 2010;54(6–7):1165–1173.

14. Scherlag BJ, Kabell G, Harrison L, Lazzara R. Mechanisms of bradycardia-induced ventricular arrhythmias in myocardial ischemia and infarction. *Circulation* 1982;65(7):1429–1434.

15. Kilani B et al. Comparison of endothelial promoter efficiency and specificity in mice reveals a subset of Pdgfb-positive hematopoietic cells. *J. Thromb. Haemost.* 2019;17(5):827–840.

16. Boulanger CM, Loyer X, Rautou P-E, Amabile N. Extracellular vesicles in coronary artery disease. *Nat Rev Cardiol* 2017;14(5):259–272.

17. van Niel G, D'Angelo G, Raposo G. Shedding light on the cell biology of extracellular vesicles. *Nat. Rev. Mol. Cell Biol.* 2018;19(4):213–228.

18. Donadee C et al. Nitric oxide scavenging by red blood cell microparticles and cell-free hemoglobin as a mechanism for the red cell storage lesion. *Circulation* 2011;124(4):465–476.

19. Camus SM et al. Circulating cell membrane microparticles transfer heme to endothelial cells and trigger vasoocclusions in sickle cell disease. *Blood* 2015;125(24):3805–3814.

20. Vanhoutte PM, Zhao Y, Xu A, Leung SWS. Thirty Years of Saying NO: Sources, Fate, Actions, and Misfortunes of the Endothelium-Derived Vasodilator Mediator. *Circ. Res.* 2016;119(2):375–396.

21. Stocker R, Keaney JF. Role of Oxidative Modifications in Atherosclerosis. *Physiological Reviews* 2004;84(4):1381–1478.

745   22. Teng N et al. The roles of myeloperoxidase in coronary artery disease and its potential implication in plaque rupture. *Redox Report* 2017;22(2):51–73.

23. Sen-Banerjee S et al. Kruppel-Like Factor 2 as a Novel Mediator of Statin Effects in Endothelial Cells. *Circulation* 2005;112(5):720–726.

24. Mason RP, Walter MF, Jacob RF. Effects of HMG-CoA reductase inhibitors on endothelial

750   function: role of microdomains and oxidative stress. *Circulation* 2004;109(21 Suppl 1):II34-41.

25. Bang OY, Toyoda K, Arenillas JF, Liu L, Kim JS. Intracranial Large Artery Disease of Non-Atherosclerotic Origin: Recent Progress and Clinical Implications. *J Stroke* 2018;20(2):208–217.

26. Neunteufl T, Heher S, Stefenelli T, Pabinger I, Gisslinger H. Endothelial dysfunction in patients with polycythaemia vera. *Br. J. Haematol.* 2001;115(2):354–359.

755   27. Charpentier A et al. Microparticle phenotypes are associated with driver mutations and distinct thrombotic risks in essential thrombocythemia. *Haematologica* 2016;101(9):e365-368.

28. Tan X et al. Role of erythrocytes and platelets in the hypercoagulable status in polycythemia vera through phosphatidylserine exposure and microparticle generation. *Thrombosis and Haemostasis* 2013;109(06):1025–1032.

760   29. Baccouche H et al. The evaluation of the relevance of thrombin generation and procoagulant activity in thrombotic risk assessment in BCR-ABL-negative myeloproliferative neoplasm patients. *Int J Lab Hematol* 2017;39(5):502–507.

30. Duchemin J et al. Increased circulating procoagulant activity and thrombin generation in patients with myeloproliferative neoplasms. *Thromb. Res.* 2010;126(3):238–242.

765   31. Marchetti M et al. Phospholipid-dependent procoagulant activity is highly expressed by circulating microparticles in patients with essential thrombocythemia. *Am. J. Hematol.* 2014;89(1):68–73.

32. Trappenburg MC et al. Elevated procoagulant microparticles expressing endothelial and

platelet markers in essential thrombocythemia. *Haematologica* 2009;94(7):911–918.

770   33. Zhang W et al. Clinical significance of circulating microparticles in Ph− myeloproliferative

neoplasms. *Oncol Lett* 2017;14(2):2531–2536.

34. Moles-Moreau M-P et al. Flow cytometry-evaluated platelet CD36 expression, reticulated

platelets and platelet microparticles in essential thrombocythaemia and secondary thrombocytosis.

Thromb. Res. 2010;126(5):e394-396.

775   35. Kissova J, Ovesna P, Bulikova A, Zavřelova J, Penka M. Increasing procoagulant activity of

circulating microparticles in patients with Philadelphia-negative myeloproliferative neoplasms: a

single-centre experience. *Blood Coagul. Fibrinolysis* 2015;26(4):448–453.

36. Musolino C et al. Changes in advanced oxidation protein products, advanced glycation end

products, and s-nitrosylated proteins, in patients affected by polycythemia vera and essential

780   thrombocythemia. *Clin. Biochem.* 2012;45(16–17):1439–1443.

37. Durmus A et al. Increased oxidative stress in patients with essential thrombocythemia. *Eur Rev

Med Pharmacol Sci* 2013;17(21):2860–2866.

38. Vener C et al. Oxidative stress is increased in primary and post-polycythemia vera

myelofibrosis. *Exp. Hematol.* 2010;38(11):1058–1065.

785   39. Hasselbalch HC et al. Whole blood transcriptional profiling reveals deregulation of oxidative

and antioxidative defence genes in myelofibrosis and related neoplasms. Potential implications of

downregulation of Nrf2 for genomic instability and disease progression. *PLoS ONE*

2014;9(11):e112786.

40. Said AS, Doctor A. Influence of red blood cell-derived microparticles upon vasoregulation.

790   *Blood Transfus* 2017;15(6):522–534.

41. Adam M et al. Red blood cells serve as intravascular carriers of myeloperoxidase. *Journal of

Molecular and Cellular Cardiology* 2014;74:353–363.

42. Gorudko IV et al. Binding of human myeloperoxidase to red blood cells: Molecular targets and biophysical consequences at the plasma membrane level. *Archives of Biochemistry and Biophysics* 2016;591:87–97.

43. Cheng David et al. Inhibition of MPO (Myeloperoxidase) Attenuates Endothelial Dysfunction in Mouse Models of Vascular Inflammation and Atherosclerosis. *Arteriosclerosis, Thrombosis, and Vascular Biology* 0(0):ATVBAHA.119.312725.

44. Benson TW et al. A single high-fat meal provokes pathological erythrocyte remodeling and increases myeloperoxidase levels: implications for acute coronary syndrome. *Laboratory Investigation* 2018;98(10):1300.

45. Baldus S et al. Myeloperoxidase enhances nitric oxide catabolism during myocardial ischemia and reperfusion. *Free Radical Biology and Medicine* 2004;37(6):902–911.

46. Angona A et al. Dynamics of JAK2 V617F allele burden of CD34+ haematopoietic progenitor cells in patients treated with ruxolitinib. *Br. J. Haematol.* 2016;172(4):639–642.

47. Vainchenker W et al. JAK inhibitors for the treatment of myeloproliferative neoplasms and other disorders. *F1000Res* 2018;7:82.

48. Boulanger CM et al. Circulating Microparticles From Patients With Myocardial Infarction Cause Endothelial Dysfunction. *Circulation* 2001;104(22):2649–2652.

49. Rautou P-E et al. Abnormal plasma microparticles impair vasoconstrictor responses in patients with cirrhosis. *Gastroenterology* 2012;143(1):166-176.e6.

50. Marty C et al. A role for reactive oxygen species in $JAK2^{V617F}$ myeloproliferative neoplasm progression. *Leukemia* 2013;27(11):2187–2195.

51. Wang Y et al. Ephrin-B2 controls VEGF-induced angiogenesis and lymphangiogenesis. *Nature* 2010;465(7297):483–486.

52. Schnütgen F, Ghyselinck NB. Adopting the good reFLEXes when generating conditional

alterations in the mouse genome. *Transgenic Res.* 2007;16(4):405–413.

53. Payancé A et al. Hepatocyte microvesicle levels improve prediction of mortality in patients with cirrhosis. *Hepatology* [published online ahead of print: March 30, 2018]; doi:10.1002/hep.29903

54. Kubovcakova L et al. Differential effects of hydroxyurea and INC424 on mutant allele burden and myeloproliferative phenotype in a JAK2-V617F polycythemia vera mouse model. *Blood* 2013;121(7):1188–1199.

55. Maschalidi S, Sepulveda FE, Garrigue A, Fischer A, de Saint Basile G. Therapeutic effect of JAK1/2 blockade on the manifestations of hemophagocytic lymphohistiocytosis in mice. *Blood* 2016;128(1):60–71.

56. Kou R, Shiroto T, Sartoretto JL, Michel T. Suppression of Gαs synthesis by simvastatin treatment of vascular endothelial cells. *J. Biol. Chem.* 2012;287(4):2643–2651.

57. Lamrani L et al. Hemostatic disorders in a JAK2V617F-driven mouse model of myeloproliferative neoplasm. *Blood* 2014;124(7):1136–1145.

58. Poullet P, Carpentier S, Barillot E. myProMS, a web server for management and validation of mass spectrometry-based proteomic data. *Proteomics* 2007;7(15):2553–2556.

59. Valot B, Langella O, Nano E, Zivy M. MassChroQ: a versatile tool for mass spectrometry quantification. *Proteomics* 2011;11(17):3572–3577.

60. Vizcaíno JA et al. 2016 update of the PRIDE database and its related tools. *Nucleic Acids Res.* 2016;44(D1):D447-456.
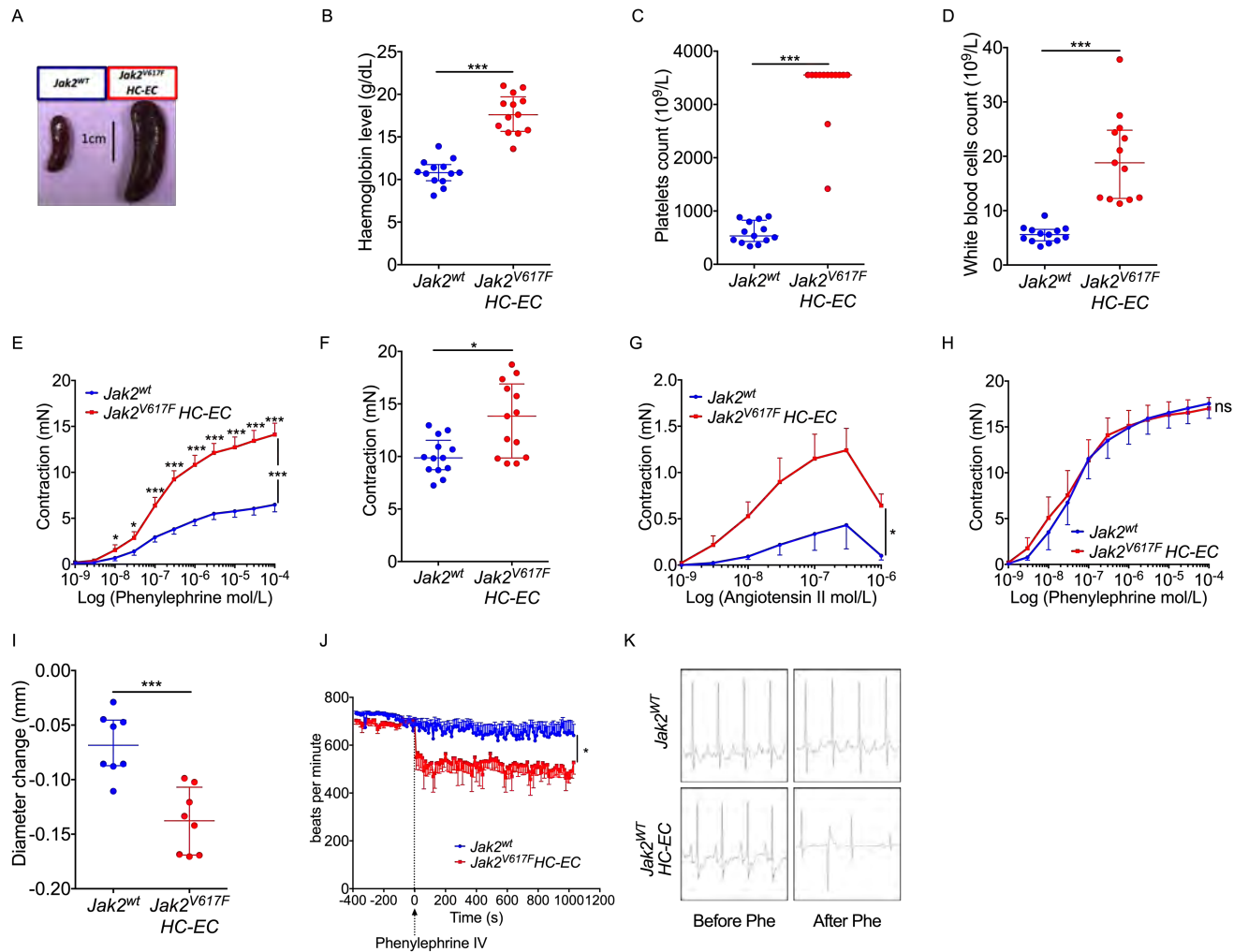
Figure 1.

Figure 1. *JAK2^{V617F} in hematopoietic and endothelial cells increases arterial contraction in an endothelial-dependent manner.*

*Representative picture of the spleen (A). Haemoglobin (B), platelet (C) and white blood cell count (D) of 8 to 12 weeks old control mice (Jak2^{WT}, n=13) and Jak2$^{V617F\ Flex/WT}$;VE-Cadherin-cre mice (Jak2^{V617F} HC-EC, n=13). Cumulative dose-response curves to phenylephrine (E) (Jak2^{WT}, n=13; Jak2^{V617F} HC-EC, n=13), to angiotensin II (G) (Jak2^{WT}, n=3; Jak2^{V617F} HC-EC, n=4) and contraction response to potassium chloride (80 mmol/L) (F) (Jak2^{WT}, n=13; Jak2^{V617F} HC-EC, n=13) of aortas with endothelium. Cumulative dose-response curves to phenylephrine of aortas without endothelium (H) (Jak2^{WT}, n=6; Jak2^{V617F} HC-EC, n=6). Diameter change of femoral artery after phenylephrine injection (10^{-3} mol/L) (I) (Jak2^{WT}, n=8; Jak2^{V617F} HC-EC, n=8). Electrocardiogram recording before and after intravenous phenylephrine injection (3 mg/kg; Jak2^{WT}, n=13; Jak2^{V617F} HC-EC, n=6) (J), with representative images of the changes observed in 5/6 Jak2^{V617F} HC-EC vs. only 4/13 Jak2^{WT} (p=0.057) (K). Quantitative data are expressed as median with interquartile range and cumulative dose-response curves are expressed as mean with standard error of the mean. Jak2^{WT} mice are in blue and Jak2^{V617F} HC-EC mice in red. Abbreviations: * p<0.05, *** p< 0.001; ns, not significant. Cumulative dose response curves and electrocardiogram recording were compared using an analysis of variance for repeated measures and other data were compared using the Mann-Whitney U-test. All tests were 2 sided.*
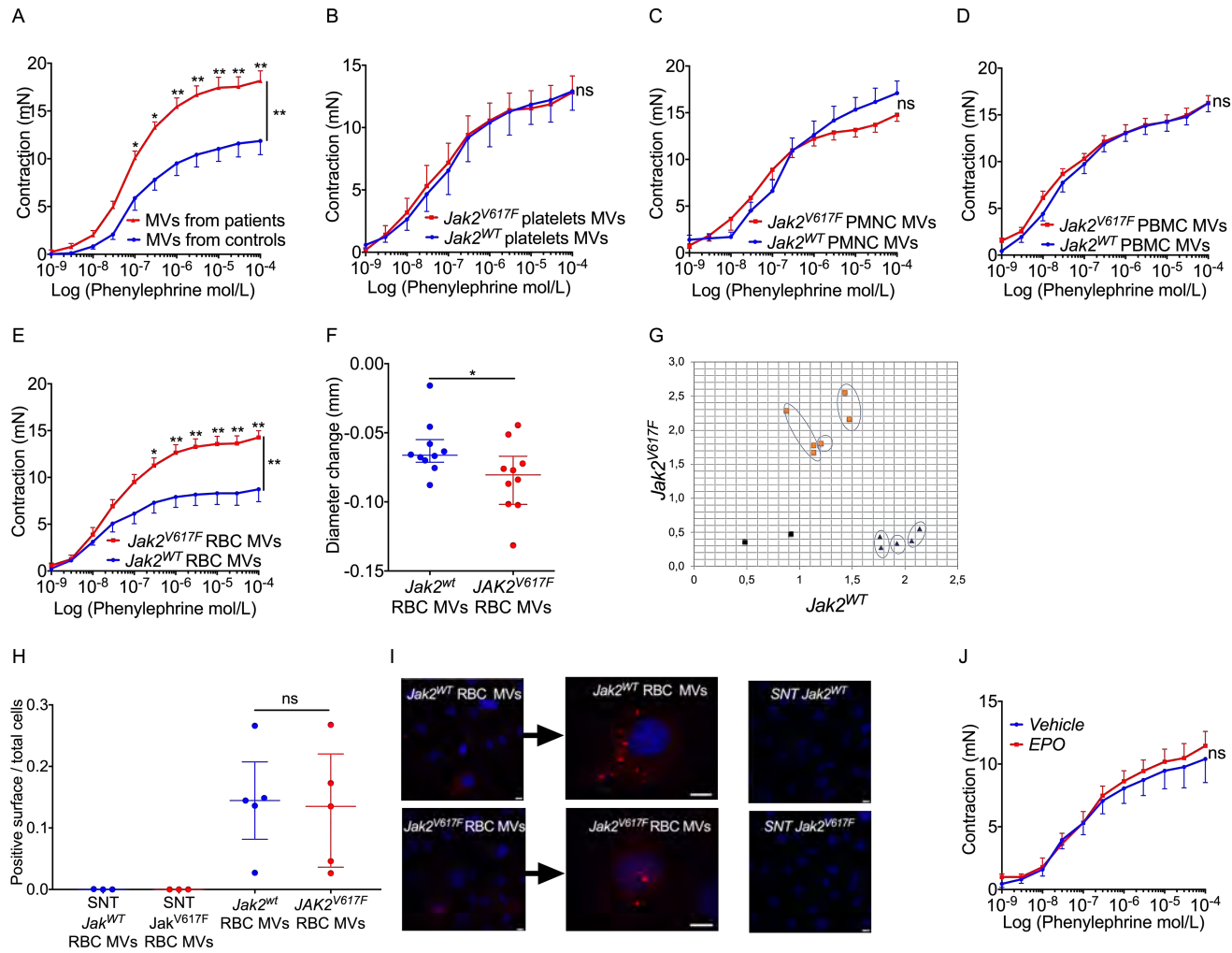
Figure 2.
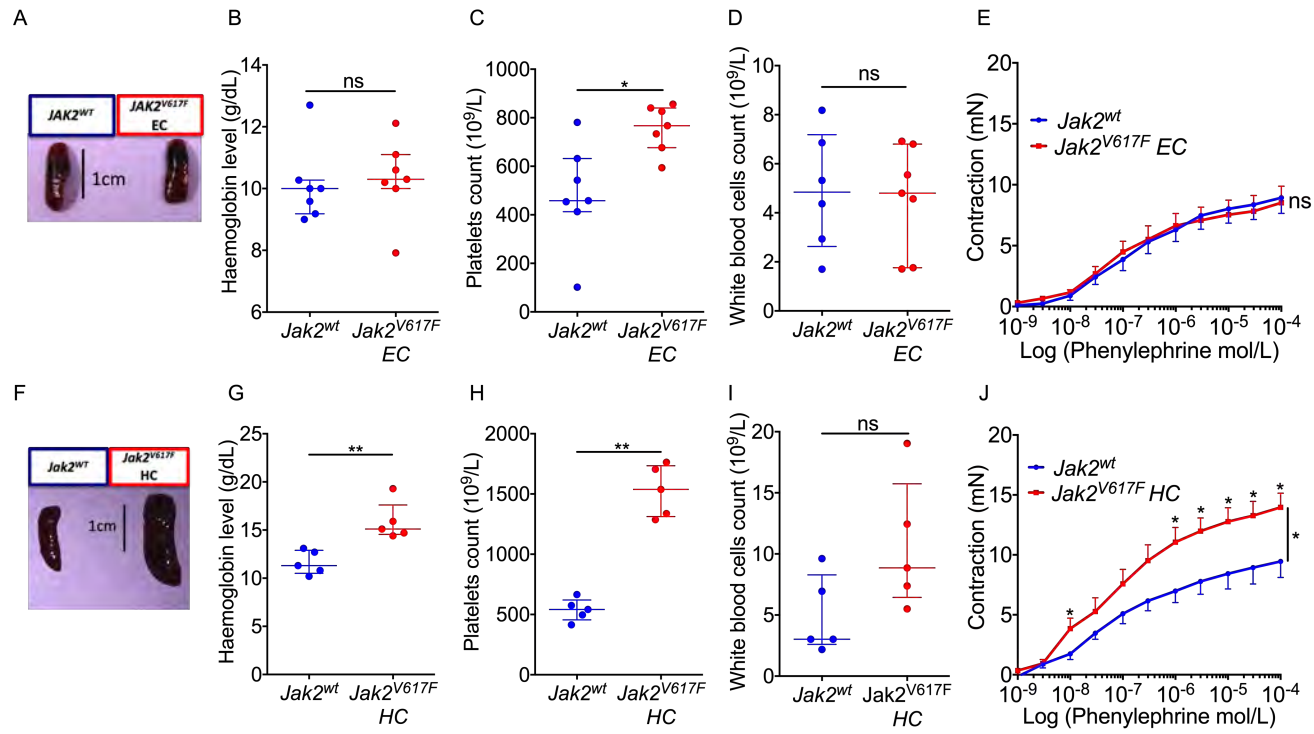
Figure 2. *JAK2^{V617F} specifically expressed in hematopoietic cells, but not in endothelial cells, increases arterial contraction*

*Representative picture of the spleen **(A and F)**. Blood cell count of 10 to 13 weeks old control mice (Jak2^{WT}, n=7, blue) and Jak2$^{V617F\ Flex/WT}$; VE-Cadherin-cre-ERT2 mice (Jak2^{V617F} EC, n=7, red) **(B, C, D)** and of 13 to 15 weeks old chimeric C57BL/6 mice transplanted with a bone marrow of wild-type mice (Jak2^{WT}, n=5, blue) or of Jak2^{V617F} HC-EC mice (Jak2^{V617F} HC, n=5, red) **(G, H I)**. Data are expressed as median with interquartile range. Cumulative dose-response curve to phenylephrine of aortas from Jak2^{WT} (n=7, blue) and Jak2^{V617F} EC (n=7, red) **(E)** and from Jak2^{WT} (n=5, blue) and Jak2^{V617F} HC (n=5, red) **(J)**. Quantitative data are expressed as median with interquartile range and cumulative dose-response curves are expressed as mean with standard error of the mean. Abbreviations: * p<0.05, ** p< 0.01; ns, not significant. Cumulative dose response curves were compared using an analysis of variance for repeated measures and other data were compared using the Mann-Whitney U-test. All tests were 2 sided.*

5

Figure 3.

Figure 3. *Microvesicles derived from JAK2^{V617F} red blood cells are responsible for an increased arterial contraction*

*Cumulative dose-response curves to phenylephrine of aortas from WT mice incubated with microvesicles isolated from JAK2^{V617F} patients (n=7, red) and controls (n=5, blue) at their circulating concentration **(A)**. Cumulative dose-response curves to phenylephrine of aortas from WT mice incubated with microvesicles generated from platelets (n=5 and n=5, respectively) **(B)**, PBMC (n=5 and n=6, respectively) **(C)**, PMNC (n=5 and n=5) **(D)** and red blood cells (n=9 and n=4, respectively) **(E)** from Jak2^{V617F} HC-EC mice (Jak2^{V617F}, red) or littermate control mice (WT, blue). Change in the diameter of femoral artery induced by phenylephrine injection (10^{-3} mol/L) in control mice previously injected with control erythrocyte-derived microvesicles (JAK2^{WT} MV GR WT, n=10, blue) or with JAK2^{V617F} erythrocyte-derived microvesicles (JAK2^{WT} MV GR Jak2^{V617F} n=10, red) **(F)**. Allelic discrimination plot of ARN isolated from microvesicles derived from Jak2^{WT} (in blue) and Jak2^{V617F} erythrocytes (in orange) (n=3 per group) (no template control, black) **(G)**. Quantification **(H)** and representative images **(I)** of the uptake by endothelial cells (HUVEC with DAPI in blue) of erythrocyte-derived microvesicles from JAK2^{V617F} mice (in red, n=5) or JAK2^{WT} mice (in blue, n=5) or respective 20500 g supernatant (n=3 for each group). Bar scale 10 μm. Cumulative dose-response curve to phenylephrine of aortas from WT mice injected with vehicle (blue, n= 5) or with epoietin (red, n=8) **(J)**. Quantitative data are expressed as median with interquartile range and cumulative dose-response curves are expressed as mean with standard error of the mean. Abbreviations: *p<0.05; ** p< 0.01; EPO, epoietin, HUVEC, Human umbilical vein endothelial cells, MVs, microvesicles; ns, not significant; NTC, no template control; PBMC, peripheral blood mononuclear cells; PMNC, polymorphonuclear cells; RBC, Red blood cells; SNT, Supernatant; WT, wild type. Cumulative dose response curves were compared using an analysis of variance for repeated measures and other data were compared using the Mann-Whitney U-test. All tests were 2 sided.*
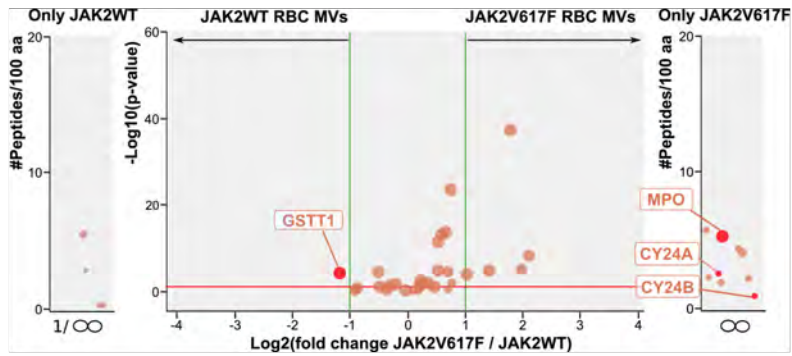
Figure 4.
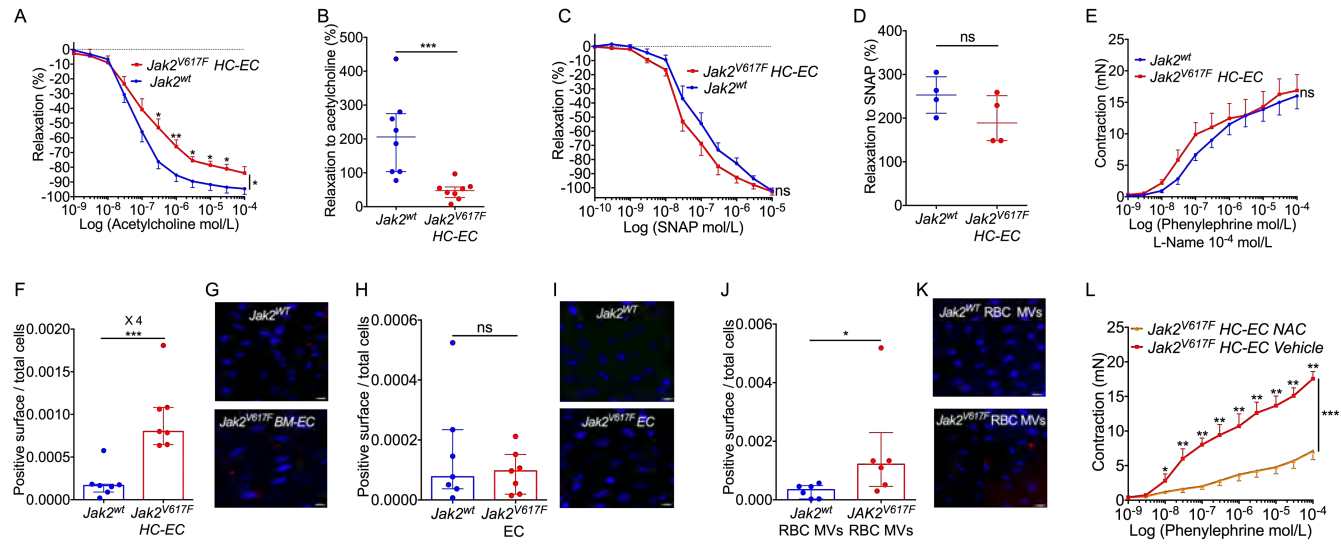
**Figure *4*. *Disturbed endothelial NO pathway and increased oxidative stress status.***

Cumulative dose-response curve of aortas from Jak2$^{V617F\,Flex/WT}$;VE-Cadherin-cre mice (Jak2^{V617F} HC-EC mice in red) and littermate controls (Jak2^{WT} in blue) to acetylcholine (n=11 and n=11, respectively) **(A),** *to S-Nitroso-N-Acetylpenicillamine (SNAP) (n=5 and n=6, respectively)* **(C)** *and to phenylephrine after L-NAME incubation (n=11 and n=7, respectively)* **(E).** *Diameter change of femoral arteries after injection of acetylcholine (10^{-2} mol/L) (Jak2^{WT}, n=8, blue; Jak2^{V617F} HC-EC, n=8, red)* **(B)** *and SNAP (10^{-3} mol/L) (Jak2^{WT}, n=4, blue; Jak2^{V617F} HC-EC, n=4, red)* **(D).** *Quantification of reactive oxygen species (ROS) generation (red surface) per endothelial cell in: control mice (Jak2^{WT}) in blue vs. Jak2^{V617F} HC-EC mice in red* **(F);** *control mice (Jak2^{WT} in blue) and Jak2$^{V617F\,Flex/WT}$;VE-Cadherin-cre-ERT2 mice (Jak2^{V617F} EC in red)* **(H);** *control mice injected with microvesicles derived from control (JAK2^{WT} MV GR WT, n=6, blue) or JAK2^{V617F} erythrocytes (JAK2^{WT} MV GR JAK2^{V617F} n=6, red)* **(J).** *Representative images of "en face" endothelial staining with CellRox® (Red fluorogenic probes for ROS generation) and DAPI (nucleus in blue) of aortas* **(G, I, K).** *Bar scale 10 μm. Cumulative dose-response curve to phenylephrine of aortas from Jak2^{V617F} HC-EC mice treated with vehicle (n=5, red) and with NAC (n=7, orange)* **(L).** *Quantitative data are expressed as median with interquartile range and compared using the Mann-Whitney U-test and cumulative dose-response curves are expressed as mean with standard error of the mean and compared using an analysis of variance for repeated measures. Abbreviations: * p<0.05, *** p< 0.001; CY24A, NAC, N-Acetyl-cysteine; ns, not significant.*
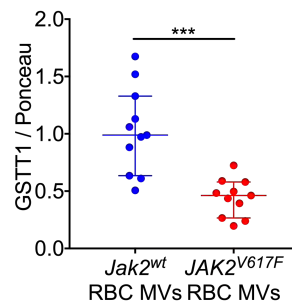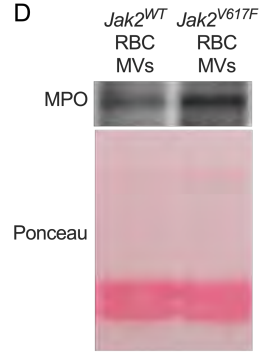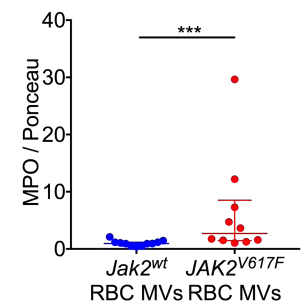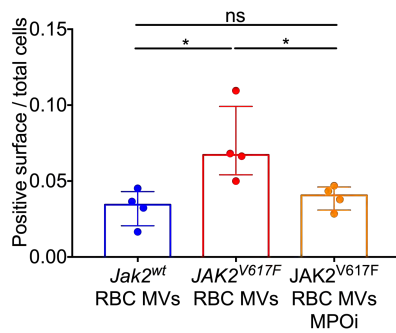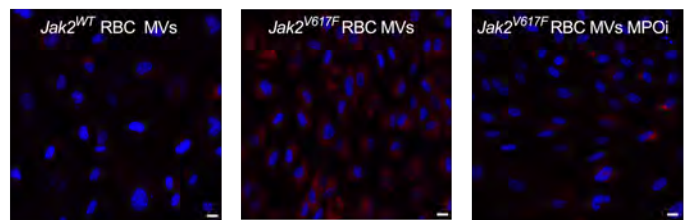
Figure 5.
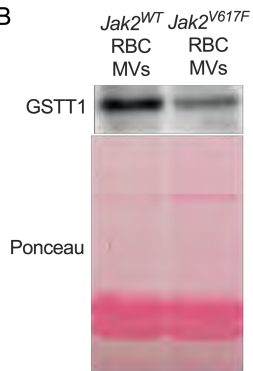
Figure 5. *Myeloperoxidase carried by erythrocyte-derived microvesicles from Jak2^{V617F} mice is responsible for increased endothelial oxidative stress.*

*Volcano plot obtained by using quantitative label-free mass spectrometry analysis of proteins isolated from microvesicles derived from JAK2^{V617F} (n=6) and JAK2^{WT} (n=4) erythrocytes (ratio JAK2^{V617F}/JAK2^{WT}) (A), only proteins involved in cellular oxidant detoxification (GO 0098869) and ROS metabolic process (GO 0072593) are presented (red line corresponds to p-value< 0.05). Representative image of GSTT1 (B) and MPO (D) western blots performed on erythrocyte-derived microvesicles, with respective quantification (C, E) (JAK2^{WT} erythrocyte microvesicles, n=11, blue; JAK2^{V617F} erythrocyte microvesicles, n=11, red). Quantification of reactive oxygen species (ROS) generation (red surface) per endothelial cell (HUVEC) after exposition of erythrocyte-derived microvesicles from control mice (Jak2^{WT}, blue) (n=4) and Jak2^{V617F} HC-EC mice and without (red, n=4) and with (orange, n=4) preincubation with a myeloperoxidase inhibitor (MPOi, PF06281355, Sigma, 5 μmol/L) (F); Representative images of HUVEC staining with CellRox® (Red fluorogenic probes for ROS generation) and DAPI (nucleus in blue) (G). Bar scale 10 μm. Quantitative data are expressed as median with interquartile range and compared using the Mann-Whitney U-test and Kruskal-Wallis test for multiple comparison. Abbreviations: * p<0.05, *** p< 0.001; CY24A, Cytochrome b-245 light chain; CY24B, Cytochrome-b245 Heavy chain; GSTT1, glutathione s transferase theta 1; MPO, myeloperoxidase; ns, not significant.*
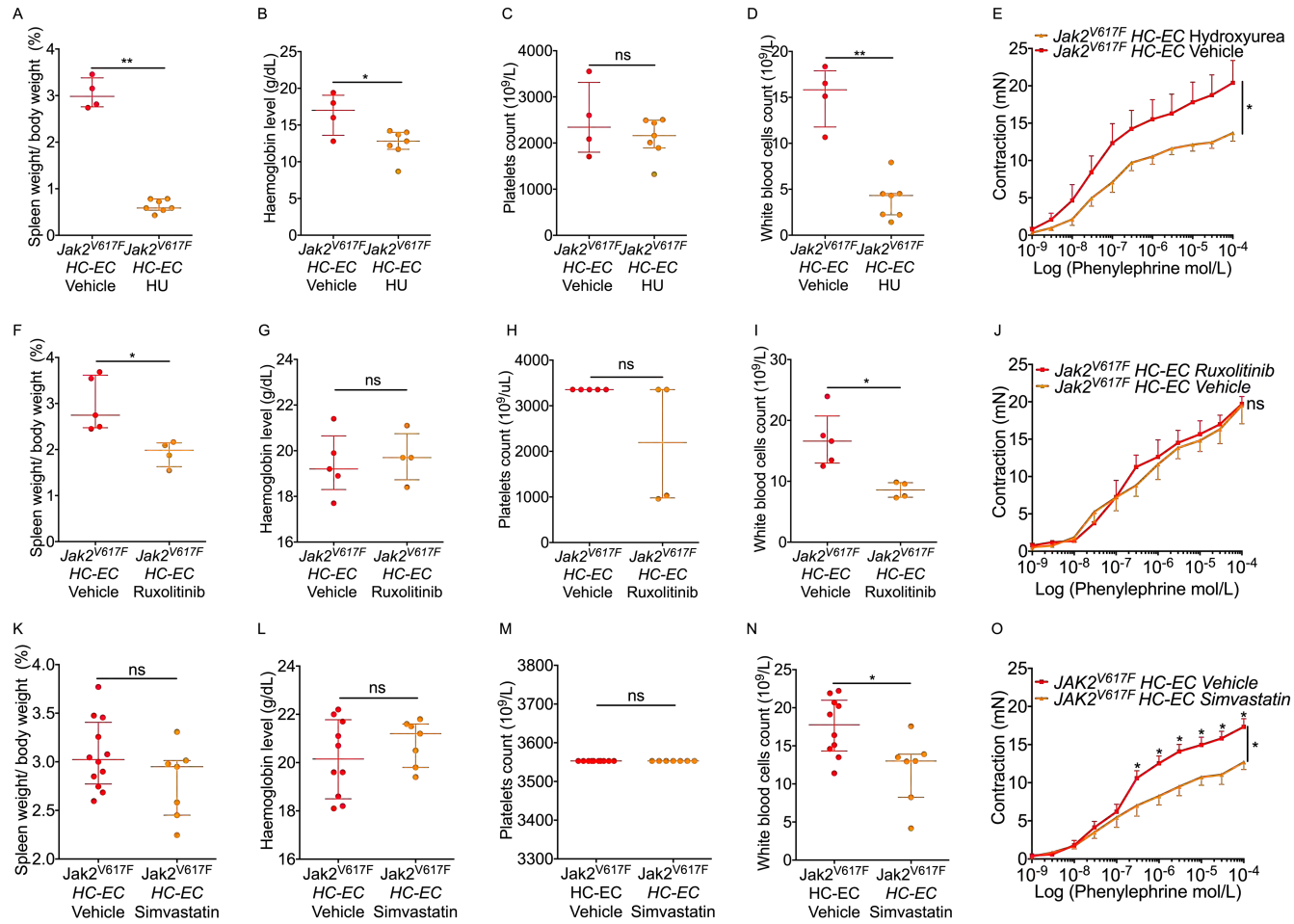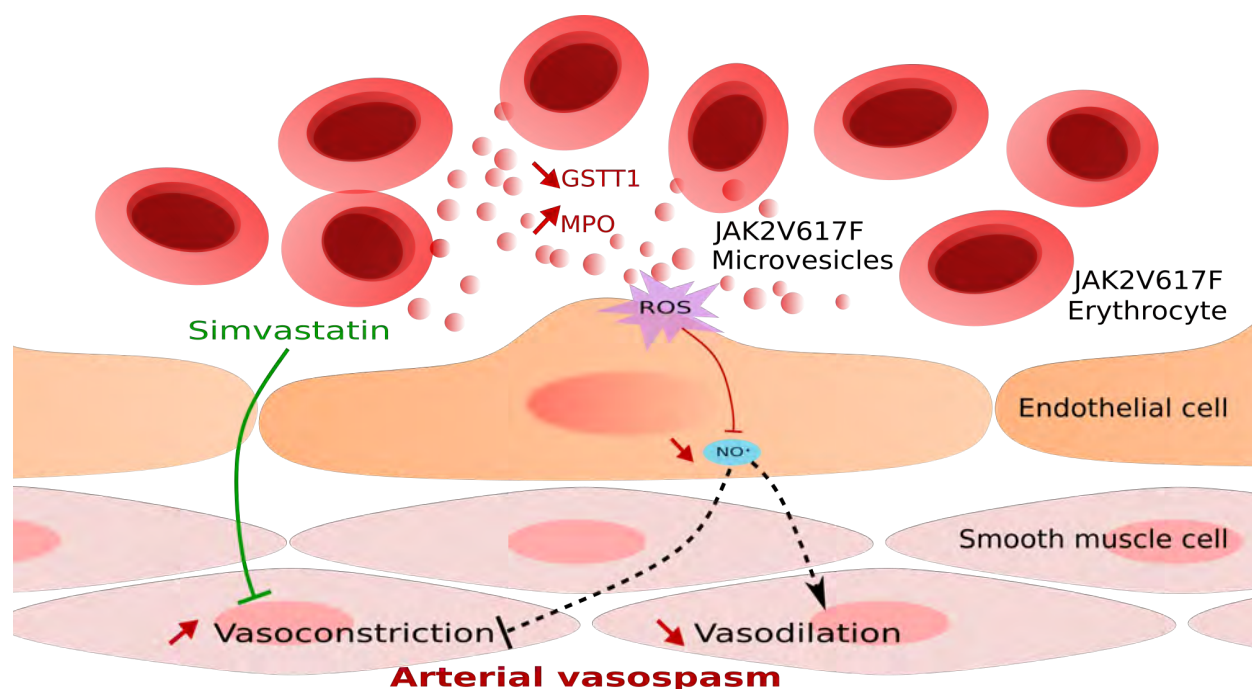
Figure 6.

Figure 6. *Simvastatin improves the increased arterial contraction induced by JAK2^{V617F}*

*Spleen to body weight ratio **(A),** haemoglobin level **(B),** platelet **(C)** and white blood cell count **(D)** in Jak2$^{V617F\ Flex/WT}$;VE-Cadherin-cre mice (Jak2^{V617F} HC-EC) treated with vehicle (Jak2^{V617F} HC-EC vehicle, red, n=4) or with hydroxyurea (Jak2^{V617F} HC-EC HU, orange, n=7). Spleen to body weight ratio **(F),** haemoglobin level **(G),** platelet **(H)** and white blood cell count **(I)** in Jak2^{V617F} HC-EC mice treated with vehicle (Jak2^{V617F} HC-EC vehicle, red, n=5) or with ruxolitinib (Jak2^{V617F} HC-EC ruxolitinib, orange, n=4). Spleen to body weight ratio **(K),** haemoglobin level **(L),** platelet **(M)** and white blood cell count **(N)** in Jak2^{V617F} HC-EC mice treated with vehicle (red, n=10) or with simvastatin (Jak2^{V617F} HC-EC simvastatin, orange, n=7).Cumulative dose-response curves to phenylephrine of aortas from Jak2^{V617F} HC-EC mice treated with vehicle or hydroxyurea (Jak2^{V617F} HC-EC vehicle in red, n=4; and Jak2^{V617F} HC-EC HU, in orange, n=7) **(E),** with vehicle or ruxolitinib (Jak2^{V617F} HC -EC vehicle in red, n= 5; and Jak2^{V617F} HC-EC Ruxolitinib in orange, n=4) **(J),** and with vehicle or simvastatin (Jak2^{V617F} HC-EC vehicle in red, n=10; and Jak2^{V617F} HC-EC simvastatin in orange, n=7) **(O).** Data are expressed as mean with standard error of the mean for cumulative curve and median with interquartile range for spleen weight and blood cell count. Abbreviations: * p<0.05, ** p< 0.01, HU hydroxyurea; ns, not significant. Cumulative dose response curves were compared using an analysis of variance for repeated measures and other data were compared using the Mann-Whitney U-test. All tests were 2 sided.*

Graphical Abstract:

Supplementary Materials:

Figures S1-S4

Table S1